

## ACKNOWLEDGMENTS

One of us (K.F.L.) wishes to thank Dr. J. L. Hirshfield and Dr. I. B. Bernstein for sending him

the paper cited in Ref. 14 prior to publication. He also wishes to acknowledge a useful correspondence with Dr. D. W. Ross.

\*Research supported by the National Science Foundation under Grant No. GK-4592.

†Research supported by NASA Contract No. DPR-R21-009-004 and U.S. Department of Navy Contract No. N00017-62-C-0604.

‡Permanent address: Applied Physics Laboratory, Johns Hopkins University, Silver Spring, Md.

<sup>1</sup>I. B. Bernstein, *Phys. Rev.* **109**, 10 (1958).

<sup>2</sup>S. Hamasaki, *Phys. Fluids* **11**, 2724 (1968).

<sup>3</sup>R. C. Davidson and C. S. Wu, *Phys. Fluids* **13**, 1407 (1970).

<sup>4</sup>K. F. Lee, *Phys. Rev. Letters* **21**, 1439 (1968).

<sup>5</sup>K. F. Lee, *Phys. Rev.* **181**, 447 (1969).

<sup>6</sup>K. F. Lee, *J. Appl. Phys.* **41**, 3045 (1970).

<sup>7</sup>M. Bornatici and K. F. Lee, *Phys. Fluids* **13**, 3007

(1970).

<sup>8</sup>N. Tzoar and T. P. Yang, *Phys. Rev. A* **2**, 2000 (1970).

<sup>9</sup>T. Stringer, *J. Nucl. Energy C* **6**, 267 (1964).

<sup>10</sup>E. N. Parker, *Phys. Rev.* **112**, 1429 (1958).

<sup>11</sup>W. E. Nexsen, Jr., F. H. Cummins, F. H. Coensgen, A. E. Sherman, *Phys. Rev.* **119**, 1457 (1960).

<sup>12</sup>D. E. Baldwin, I. B. Bernstein, and M. P. H. Weenink, in *Advances in Plasma Physics*, edited by A. Simon and W. B. Thompson (Interscience, New York, 1969), Vol. 3, p. 32.

<sup>13</sup>K. F. Lee and J. C. Armstrong, *Phys. Rev. Letters* **26**, 77 (1971); **26**, 805 (1971).

<sup>14</sup>J. L. Hirshfield and I. B. Bernstein (unpublished).

<sup>15</sup>T. H. Stix, *The Theory of Plasma Waves* (McGraw-Hill, New York, 1962), p. 113

## Low-Frequency Instabilities in Magnetic Pulses

Nicholas A. Krall and Paulett C. Liewer

*Department of Physics and Astronomy, University of Maryland,  
College Park, Maryland 20740*

(Received 17 June 1971)

Electrons drifting relative to ions across a magnetic field are found to drive a set of intermediate-frequency long-wavelength waves ( $\omega_{ci} < \omega < \omega_{ce}$ ) unstable for any temperature ratio  $T_e/T_i$ . One instability is caused by the coupling of a drift wave in a nonuniform plasma to either the ion plasma oscillation or a lower hybrid oscillation, depending on density and field strength. Another instability is a form of the two-stream instability, shown here to exist even for drift speeds less than electron thermal speeds. Growth rates are on the order of the ion plasma (or lower hybrid) frequency, depending on the density and field strength.

### I. INTRODUCTION AND SUMMARY

Ion-acoustic-wave instabilities have been widely invoked to explain the large resistivity observed in fast  $\theta$ - and  $Z$ -pinch experiments<sup>1-4</sup> and especially to explain the widths of collisionless shock waves which often form in these experiments.<sup>5-9</sup> A recurrent difficulty with explanations in terms of ion sound instabilities is that they typically require  $T_e/T_i \geq 10$  in order for the growth of the instability to be fast enough to affect the experiment. This generally requires that some mechanism be proposed to preheat the electrons; often little evidence exists for such preheating.<sup>3, 4, 10</sup>

In this paper, we demonstrate that the plasma configurations typically found in  $\theta$ - and  $Z$ -pinch plasmas are unstable to various intermediate-frequency ( $\omega_{ci} < \omega < \omega_{ce}$ ) long-wavelength waves even for  $T_e < T_i$ . One instability is caused by a coupling of ion plasma or lower hybrid oscillations to drift waves in a nonuniform plasma. Another is a modified electron-ion streaming instability, which

grows even when the stream is subthermal. Both are nonresonant fluidlike branches of resonant particle instabilities previously explored.<sup>6, 8, 9</sup> The existence of these modes has been shown previously using the cold-fluid hydrodynamic equations<sup>11</sup>; the present treatment emphasizes their behavior in a warm magnetoplasma treated through the Vlasov equation, showing especially the dependence of the modes on the size and direction of magnetic, density, and temperature gradients in the plasma.

In Sec. II, we derive the dispersion relation for electrostatic waves in a plasma equilibrium appropriate to magnetic shock and diffusion experiments. This equilibrium is magnetically confined [ $\vec{B} = B(r)\hat{z}$ ], inhomogeneous [ $n_e T_e = n_e(r)T_e(r)$ ], and, in general, includes an electric field perpendicular to the magnetic field [ $\vec{E} = E_0\hat{r}$ ]. It is assumed that this electric field drives a drift ( $v_E = cE_0/B$ ) in the electrons, but because of the time scale or some other feature of the experiment, does not affect the ions.

In Sec. III, we treat analytically two distinct

types of instability: (a) flutelike drift modes. If both the electric field  $E_0$  and a gradient in  $n_e$ ,  $T_{\perp e}$ , or  $B$  are retained, we find that the plasma is unstable to a flutelike wave, propagating across the field, of frequency and growth rate

$$\omega_R \approx \omega_{pi}(1 + 4\pi n m c^2 / B^2)^{-1/2}, \quad \gamma \approx \sqrt{2} \omega_R,$$

where  $m$  is the electron mass and  $\omega_{pi}$  is the ion plasma frequency. The condition for this strong instability is that the particle drifts and currents not be too weak:

$$v_{\Delta} v_E \gtrsim c_s^2,$$

where

$$v_E = cE_0/B,$$

$$v_{\Delta} = -\frac{T_e}{m\omega_{ce}} \left( \frac{1}{n_e} \frac{dn_e}{dx} - \frac{1}{B} \frac{dB}{dx} - \frac{k_{\perp}^2 a_e^2}{2} \frac{1}{T_e} \frac{dT_{\perp e}}{dx} \right),$$

with  $\omega_{ce}$ , the cyclotron frequency of electrons ( $\omega_{ce} = |eB/mc|$ );  $a_e$ , the electron gyroradius; and  $c_s^2 = T_e/M$ , the ion sound speed with  $M$  the ion mass. This instability grows even when  $T_e < T_i$ , in contrast with other calculations of instabilities in this frequency range which look only at ion sound waves,<sup>8,9</sup> and either neglect the gradients in  $n_e$  and  $T_{\perp e}$ <sup>7,8,9</sup> or concentrate on resonant particle instabilities.<sup>6</sup> If the plasma pressure is homogeneous and the magnetic gradient is balanced by the  $cE_0/B$  current, this strong nonresonant mode stabilizes at high  $\beta = 4\pi n T_e / B^2 \gtrsim 0.02$ . (b) modified two-stream instability. Even if the gradients in  $n_e$ ,  $T_{\perp e}$ , and  $B$  are neglected, a two-stream instability persists for modes with a small component of  $\vec{k}$  parallel to the magnetic field. This long-wavelength ( $k_{\perp} a_e < 1$ ) mode propagating almost perpendicular to  $B_0$  sees the electrons, tied to the field lines, as a *cold* fluid, and is unstable as long as

$$v_E > [(T_e + T_i)/M]^{1/2}.$$

Frequency and growth rates are given by

$$\omega_R \approx \gamma_{\max} \approx \omega_{pi}(1 + 4\pi n m c^2 / B^2)^{-1/2} (v_E / c_s)^{1/5}.$$

In Sec. IV, we present numerical results for the frequency and growth rate of the drift instability for a variety of parameters. These results agree well with the analytic results of Sec. III, but extend the calculation into ranges where no analytic results can be obtained.

In Sec. V, we discuss the types of experiments to which these results can be applied.

## II. DISPERSION RELATION FOR UNSTABLE WAVES

The plasma equilibrium we consider is typical of that found in various  $\theta$ -pinch experiments and, indeed, in most magnetically confined plasma. All of these plasmas include regions of nonuniform density supported by magnetic field gradients, which

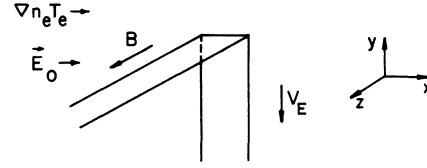


FIG. 1. Slab geometry.

for simplicity, we treat in a slab geometry. The plasma is considered as shown in Fig. 1, to be infinite and uniform in the  $y$ - $z$  plane; all equilibrium variations are in the  $x$  direction. A linear approximation is made to the changes in the magnetic field, density, and temperature perpendicular to  $B$ :

$$\vec{B}(x) = B(1 - \epsilon x)\hat{z}, \quad n_e(x) = n_e(1 - \delta x),$$

$$T_{\perp e}(x) = T_e(1 - \alpha x).$$

In the class of experiments we consider, the plasma also supports an electric field in the  $x$  direction

$$\vec{E}_0 = E\hat{x}.$$

It is assumed that  $E$  drives an *electron* current with velocity  $cE/B$ , but that the ions are not affected by the electric or magnetic fields. This assumption restricts the stability analysis to frequencies well above the ion gyrofrequency and also restricts the application of the theory to experiments where some feature prevents the electrons and ions from acquiring equal drifts  $cE/B$ . For example, in magnetic-shock and diffusion experiments, the ions do not acquire a drift because of the time scales involved: The ion-cyclotron time is longer than the time scale on which  $E$  forms, excites instability and decays. Figure 2 shows the typical situation in magnetic-shock-wave experiments.<sup>12</sup>

Thus, we take the equilibrium distribution for the electrons to be a local Maxwellian with a uniform electric field  $E\hat{x}$  and weak gradients in density and temperature:

$$f_{0e} = n_0 \left[ 1 + \left( \epsilon' + \frac{\alpha m v_{\perp}^2}{2T_e} \right) \left( \frac{v_y}{\omega_{ce}} - x \right) \right] \times \left( \frac{m}{2\pi T_e} \right)^{3/2} \exp \left[ - \left( \frac{mv^2}{2} + eEx \right) / T_e \right],$$

where  $v_{\perp}^2 = v_x^2 + v_y^2$ , while the ion distribution is treated as a simple Maxwellian distribution at rest:

$$f_{0i} = n_0 (M/2\pi T_i)^{3/2} e^{-Mv^2/2T_i}.$$

The electron density gradient is

$$\frac{1}{n_e} \frac{dn_e}{dx} = -\epsilon' - \frac{eE}{T_e} - \alpha,$$

while the temperature gradient is

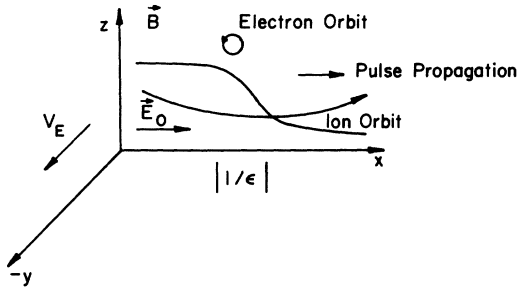


FIG. 2. Magnetic profile of a pulse propagating into the plasma. Drift velocities are perpendicular to both the magnetic and electric fields. Density and temperature also have gradients in the  $x$  direction.

$$\frac{1}{T_e} \frac{dT_{\perp e}}{dx} = -\alpha.$$

Maxwell's equation

$$\nabla \times \vec{B} = \frac{4\pi}{c} e \int d\vec{v} \vec{v} (f_{0i} - f_{0e})$$

gives for the above distributions

$$k^2 = -\frac{4\pi ne^2}{T_i} \left\{ 1 + \frac{\omega}{k} \left( \frac{M}{2T_i} \right)^{1/2} Z \left[ \frac{\omega}{k} \left( \frac{M}{2T_i} \right)^{1/2} \right] \right\} - \frac{4\pi ne^2}{T_e} + \frac{4\pi ne^2}{T_e} \left( \frac{m}{2\pi T_e} \right)^{3/2} \sum_{l=-\infty}^{\infty} 2\pi \int v_{\perp} dv_{\perp} \int dv_{\parallel} \\ \times \left\{ \left[ \omega - \frac{k_y T_e}{m\omega_{ce}} \left( \epsilon' + \alpha \frac{mv_{\perp}^2}{2T_e} \right) \right] / \left( \omega - k_y v_d - k_x v_x - l\omega_{ce} \right) \right\} J_l^2 \left( \frac{k_{\perp} v_{\perp}}{\omega_{ce}} \right) \exp \left( -\frac{mv_{\parallel}^2}{2T_e} \right), \quad (3)$$

where  $Z$  is the plasma dispersion function

$$Z(\lambda) \equiv \frac{1}{(\pi)^{1/2}} \int_{-\infty}^{\infty} e^{-x^2} \frac{dx}{(x-\lambda)}$$

The drift velocity  $v_d$  in (3) has two contributions; one is from the  $\nabla B$  drift and one is from the  $E \times B$  drift

$$v_d = \frac{\epsilon v_{\perp}^2}{2\omega_{ce}} - \frac{cE}{B}.$$

Both are in the  $y$  direction.

In the derivation several other approximations have been made. We have made the local approximation,<sup>14,15</sup> treating the gradients as weak and then expanding about  $x=0$ . The equilibrium electric field has been treated as uniform, so we require it to be constant over at least a wavelength. The perturbations were treated as pure electrostatic

$$\frac{1}{B} \frac{dB}{dx} = \frac{4\pi n T_e}{B^2} (\epsilon' + 2\alpha) = \beta(\epsilon' + 2\alpha). \quad (1)$$

The equilibrium current across the magnetic field is given by

$$v_c = \frac{1}{n_0} \int f_{0e} v_y dv_y = (\epsilon' + 2\alpha) \frac{T_e}{m\omega_{ce}} \\ = -\frac{T_e}{m\omega_{ce}} \left( \frac{1}{n_e T_e} \frac{dn_e T_{\perp e}}{dx} \right) - \frac{cE}{B}. \quad (2)$$

Part of this electron current is due to the  $E \times B$  drift,  $\vec{v}_E = -(cE/B)\hat{y}$ , and part is due to the gradient in pressure. We now assume that this equilibrium is perturbed by an electrostatic wave

$$\delta \vec{E} = \delta \vec{E} e^{i(\vec{k} \cdot \vec{x} - \omega t)}$$

of frequency  $\omega \gg \omega_{ci}$ , so that the ion response to the wave can be calculated neglecting the magnetic field  $B$ . The time development of the perturbation is given by the Vlasov-Maxwell equations; the calculation, leading to a dispersion relation for  $\omega(k)$  is done by techniques used in previous calculations,<sup>13</sup> with the familiar result

(assuming  $\delta \vec{E} = -\nabla \delta \phi$ ), which restricts Eq. (3) to  $\beta \ll 1$  in which limit neglect of perturbed magnetic fields is justified.<sup>16</sup>

It is well known that if the gradients in  $n_e$ ,  $B$ , and  $T_e$  are neglected, the dispersion relation (3) describes only short-wavelength high-frequency ( $\omega > \omega_{ce}$ ) waves propagating perpendicular to the magnetic field<sup>17-19</sup> and unstable ion-acoustic waves<sup>6-9</sup> which require  $T_e \gg T_i$ . By retaining any of the gradients  $dn_e/dx$ ,  $dT_{\perp e}/dx$ ,  $dB/dx$ , or a small component  $k_x$  parallel to  $B$ , a low-frequency long-wavelength ( $\omega_{ci} < \omega < \omega_{ce}$ ,  $k_{\perp} a_e < 1$ ) branch opens up which is unstable for any  $T_e/T_i$ .

Restricting our attention to these low-frequency long-wavelength modes  $\omega \ll \omega_{ce}$ , we keep only the  $l=0$  term in the sum.

With this limitation, the starting equation for analysis of the stability of the plasma equilibrium common to the  $\theta$  pinch and other systems becomes

$$k^2 \lambda_D^2 = -\frac{T_e}{T_i} \left\{ 1 + \frac{\omega}{k} \left( \frac{M}{2T_i} \right)^{1/2} Z \left[ \frac{\omega}{k} \left( \frac{M}{2T_i} \right)^{1/2} \right] \right\} - 1 + \frac{m}{T_e} \left( \frac{m}{2\pi T_e} \right)^{1/2} \int_{-\infty}^{\infty} dv_{\parallel} \int_0^{\infty} dv_{\perp} v_{\perp} \left\{ \left[ \omega - \frac{k_y T_e}{m\omega_{ce}} \left( \epsilon' + \alpha \frac{mv_{\perp}^2}{2T_e} \right) \right] / \right.$$

$$\left( \omega + k_y \frac{cE}{B} - \frac{k_y \epsilon v_{\perp}^2}{2\omega_{ce}} - k_x v_x \right) \left\{ J_0^2 \left( \frac{k_{\perp} v_{\perp}}{\omega_{ce}} \right) \exp \left( -\frac{m(v_{\perp}^2 + v_x^2)}{2T_e} \right) \right\}, \quad (4)$$

where  $k_{\perp}^2 = k_x^2 + k_y^2$ .

In the uniform magnetic field zero-temperature limit  $[(1/B)dB/dx \rightarrow 0, T_e \rightarrow 0, T_i \rightarrow 0]$  Eq. (4) reduces to the hydrodynamic equation for waves in a cold plasma of nonuniform density explored previously.<sup>11</sup> In Secs. III and IV, we solve (4) analytically in a variety of limiting cases and numerically for  $k_x = 0$  and  $\alpha = 0$ . The numerical solutions contain fully the effect of ion and electron temperature, through the plasma dispersion function  $Z$ .

### III. ANALYTIC RESULTS

#### A. Drift Modes, $k_x = 0$

Examples of modes resonant with the magnetic gradient drifts have been studied elsewhere<sup>6,13</sup> and require  $T_e \gg T_i$  for instability. Therefore we treat

$$\left( \frac{m}{T_e} \right) \int \frac{dv_{\perp} v_{\perp} \left[ \omega - \frac{k_y T_e}{m\omega_{ce}} \left( \epsilon' + \alpha \frac{mv_{\perp}^2}{2T_e} \right) \right] J_0^2 \left( \frac{kv_{\perp}}{\omega_{ce}} \right) \exp \left( -\frac{mv_{\perp}^2}{2T_e} \right)}{\omega + k_y \frac{cE}{B} - \frac{k_y \epsilon v_{\perp}^2}{2\omega_{ce}}} \approx \left( 1 + \frac{\frac{k_y T_e}{m\omega_{ce}} \left\{ \frac{1}{n_e} \frac{dn_e}{dx} - \left[ 1 - b \left( 1 - \frac{I_1(b)}{I_0(b)} \right) \right] \frac{1}{B} \frac{dB}{dx} - \frac{1}{T_e} \frac{dT_{\perp e}}{dx} \left( b - b \frac{I_1(b)}{I_0(b)} \right) \right\}}{\omega + \frac{k_y cE}{B}} \right) I_0(b) e^{-b}.$$

$I_0$  and  $I_1$  are modified Bessel functions of argument  $b = \frac{1}{2} k^2 a_e^2$ .

Assuming the ion thermal velocity is small compared to the phase velocity of the wave ( $\omega^2 M / 2T_i k^2 \ll 1$ ), the ion contribution in (4) can be approximated by

$$k^2 \lambda_D^2 \approx k^2 \lambda_D^2 \frac{\omega_{p1}^2}{\omega^2} - 1 + I_0(b) e^{-b}$$

$$+ \frac{k_y T_e}{m\omega_{ce}} \left\{ \frac{1}{n_e} \frac{dn_e}{dx} - \frac{1}{B} \frac{dB}{dx} \left[ 1 - b \left( 1 - \frac{I_1(b)}{I_0(b)} \right) \right] - \frac{1}{T_e} \frac{dT_{\perp e}}{dx} \left[ b - \frac{bI_1(b)}{I_0(b)} \right] \right\} I_0(b) e^{-b} / (\omega - k_y v_E). \quad (6)$$

Expanding the Bessel function for  $b = \frac{1}{2} k^2 a_e^2 \ll 1$  and using the identity  $a_e^2 / 2\lambda_D^2 = 4\pi n m c^2 / B^2$ , (4) becomes

$$(\omega - k_y v_E) \left[ \frac{\omega^2}{\omega_{p1}^2} \left( 1 + \frac{4\pi n m c^2}{B^2} \right) - 1 \right] = -\frac{k_y v_{\Delta}}{k^2 \lambda_D^2} \frac{\omega^2}{\omega_{p1}^2}, \quad (7)$$

where  $v_E = -cE/B$  is the  $E \times B$  drift velocity and

$$v_{\Delta} = -\frac{T_e}{m\omega_{ce}} \left[ \frac{1}{n_e} \frac{dn_e}{dx} - \frac{1}{B} \frac{dB}{dx} - \frac{k^2 a_e^2}{2} \frac{1}{T_e} \frac{dT_{\perp e}}{dx} \right]. \quad (8)$$

the magnetic gradient drift as weak,

$$\left| \omega + \frac{k_y cE}{B} \right| \gg \left| k_y \frac{1}{B} \frac{dB}{dx} \frac{v_{\perp}^2}{2\omega_{ce}} \right|, \quad (5)$$

and expand the denominator in (4) around

$$\epsilon = -\frac{1}{B} \frac{dB}{dx} = 0.$$

From (1) and (2) it can be seen that for  $|v_c| \sim |cE/B|$ :

$$\left| \frac{1}{B} \frac{dB}{dx} \frac{v_{\perp}^2}{2\omega_{ce}} \right| \sim \left| \frac{1}{B} \frac{dB}{dx} \frac{T_e}{m\omega_{ce}} \right| \sim \left| \beta \frac{cE}{B} \right|,$$

so (5) is equivalent to a low- $\beta$  approximation. Neglecting all products of gradients, the electron integral in (4) then becomes, with  $k_x = 0$ ,

$$-\frac{T_e}{T_i} \left\{ 1 + \frac{\omega}{k} \left( \frac{M}{2T_i} \right)^{1/2} Z \left[ \frac{\omega}{k} \left( \frac{M}{2T_i} \right)^{1/2} \right] \right\} \approx k^2 \lambda_D^2 \frac{\omega_{p1}^2}{\omega^2},$$

where  $\lambda_D$  is the electron Debye length

$$\lambda_D^2 = T_e / 4\pi n e^2.$$

The dispersion relation then becomes

From (7) it can be seen that if  $v_{\Delta} = 0$  the dispersion relation (7) would yield a stable drift wave

$$\omega = k_y v_E$$

and a stable oscillation

$$\omega^2 = \omega_{p1}^2 \left( 1 + \frac{4\pi n m c^2}{B^2} \right)^{-1} \approx \omega_{p1}^2, \quad B^2 \gg 4\pi n m c^2 \\ \approx \omega_{HB}^2, \quad B^2 \ll 4\pi n m c^2$$

where  $\omega_{\text{HB}} = eB/(Mm)^{1/2}c$  is the lower hybrid frequency. The gradients couple these two stable modes.

### 1. Weak Drift, $v_E v_\Delta \ll c_s^2$

When the drift velocity and the gradients satisfy the condition  $v_E v_\Delta \ll c_s^2$ , the solution to (7) is an unstable drift wave  $\omega \simeq k_y v_e \pm i\gamma$ . Equation (7) can be solved by expanding about  $\omega = k_y v_E + \delta$  and dropping terms of order  $\delta^3$ . Maximum growth occurs roughly when  $\delta$  is pure imaginary. This occurs when

$$\begin{aligned} k_y \lambda_D &\simeq \frac{c_s}{v_E} \left(1 + \frac{4\pi n m c^2}{B^2}\right)^{-1/2} \left[1 - 2 \left(\frac{k_y}{k}\right)^2 \frac{v_\Delta v_E}{c_s^2}\right]^{1/2} \\ &\simeq \frac{c_s}{v_E} \left(1 + \frac{4\pi n m c^2}{B^2}\right)^{-1/2}. \end{aligned} \quad (9)$$

The frequency and growth rate are given by

$$\omega_R = k_y v_E \simeq \omega_{\text{pi}} \left(1 + \frac{4\pi n m c^2}{B^2}\right)^{-1/2} \quad (10)$$

and

$$\begin{aligned} \gamma_{\text{max}} &\simeq \omega_{\text{pi}} \left(1 + \frac{4\pi n m c^2}{B^2}\right)^{-1/2} \\ &\times \left(\frac{k_y}{k}\right) \left(\frac{1 - 2(k_y/k)^2 v_\Delta v_E / c_s^2}{1 - 3(k_y/k)^2 v_\Delta v_E / c_s^2} \frac{v_E v_\Delta}{c_s^2}\right)^{1/2} \\ &\simeq \omega_{\text{pi}} \left(1 + \frac{4\pi n m c^2}{B^2}\right)^{-1/2} \left(\frac{k_y}{k}\right) \left(\frac{v_E v_\Delta}{c_s^2}\right)^{1/2}. \end{aligned} \quad (11)$$

Various combinations of density, temperature, and field gradients can be included in (11) by making appropriate substitutions in

$$\begin{aligned} v_\Delta &= -\frac{T_e}{m\omega_{ce}} \left(\frac{1}{n} \frac{dn}{dx} - \frac{1}{B} \frac{dB}{dx}\right) \\ &- \frac{T_e}{m\omega_{ce}} \left(\frac{1}{n} \frac{dn}{dx} - \frac{1}{B} \frac{dB}{dx} - \frac{k^2 a_e^2}{2} \frac{1}{T_e} \frac{dT_{\perp e}}{dx}\right) \end{aligned}$$

using the  $ka_e$  given in (9).

From the expression for  $\gamma_{\text{max}}$ , it can be seen that there will be growth only if  $v_\Delta v_E > 0$ ; otherwise the frequency would be real. Using (1) and (2) to write

$$v_E = \frac{T_e}{m\omega_{ce}} \left(\frac{1}{n_e T_e} \frac{dn_e T_e}{dx} + \frac{1}{\beta} \frac{1}{B} \frac{dB}{dx}\right)$$

this condition becomes for a low- $\beta$  plasma

$$\begin{aligned} \left(\frac{1}{B} \frac{dB}{dx}\right)^2 - \left(\frac{1}{n} \frac{dn}{dx}\right) \left(\frac{1}{B} \frac{dB}{dx}\right) \\ + \frac{k^2 a_e^2}{2} \left(\frac{1}{T_e} \frac{dT_{\perp e}}{dx}\right) \left(\frac{1}{B} \frac{dB}{dx}\right) > 0. \end{aligned}$$

In the absence of a density gradient or in the many cases in which

$$\frac{1}{T_e} \frac{dT_{\perp e}}{dx} \gg \frac{1}{n_e} \frac{dn_e}{dx}$$

(see e.g., Ref. 20), the plasma will be most un-

stable if the temperature and magnetic gradients are in the same direction. This is the usual situation in magnetic-pulse experiments where the pulse heats the plasma as it passes through. When the density gradient is larger than the magnetic and temperature gradients, it can be seen that the density and magnetic gradients must be in opposite directions for the instability. This situation occurs down stream from magnetic-shock waves and in many other experimental configurations.<sup>21</sup>

When the magnetic gradient is sufficiently larger than the density gradient, the plasma will always be unstable for low  $\beta$ .

The approximation  $\frac{1}{2} k^2 a_e^2 < 1$ , from the expression for  $k_y$  in Eq. (9), requires simply that  $v_E > c_s$ . Neglect of finite-ion-temperature effects will be justified if  $v_E > v_i$  where  $v_i = (T_i/M)^{1/2}$  is the ion thermal speed. Therefore  $v_E > [(T_e + T_i)/M]^{1/2}$  is required for the instability.

### 2. Strong Drift, $v_E v_\Delta \gtrsim c_s^2$

When the gradients and drift velocity are stronger, satisfying  $v_E v_\Delta \gtrsim c_s^2$ , the growth rate becomes large, and the analytic expressions (9)–(11) are no longer valid. For  $\omega_R \sim \gamma$ , (7) can be solved by writing  $\omega = \omega_R + i\gamma$  and breaking (7) into real and imaginary parts. The imaginary equation can be solved for  $\gamma$  as a function of  $\omega_R$ ; the real equation can then be solved by expanding

$$\omega_R = \omega_{\text{pi}} \left(1 + \frac{4\pi n m c^2}{B^2}\right)^{-1/2} (1 + \delta) \quad (12)$$

and keeping terms linear in  $\delta$ . The maximum growth of the instability occurs when

$$k \simeq \frac{1}{\lambda_D} \left(1 + \frac{4\pi n m c^2}{B^2}\right)^{-1/2} \left(\frac{v_\Delta}{v_E}\right)^{1/2} \quad (13)$$

and

$$\delta = \frac{1}{22} \left[-6 + \frac{k_y}{k} \left(\frac{v_\Delta v_E}{c_s^2}\right)^{1/2}\right].$$

The maximum growth rate is

$$\begin{aligned} \gamma_{\text{max}} &\simeq \left[3\omega_R^2 - \omega_{\text{pi}}^2 \left(1 + \frac{4\pi n m c^2}{B^2}\right)^{-1}\right]^{1/2} \\ &\simeq \sqrt{2} \omega_{\text{pi}} \left(1 + \frac{4\pi n m c^2}{B^2}\right)^{-1/2}. \end{aligned} \quad (14)$$

As in the weak-drift case the instability requires  $v_\Delta v_E > 0$ .

The approximation  $\frac{1}{2} k^2 a_e^2 \ll 1$  requires, from (13) that  $v_\Delta/v_E \ll 1$ . For this analytic result,

$$\left(\frac{k v_i}{\omega}\right)^2 \simeq \frac{T_i}{T_e} \frac{v_\Delta}{v_E},$$

so for  $v_\Delta < v_E$ , neglect of finite ion temperature will be valid even for  $T_e \lesssim T_i$ .

Note from (9)–(11) and (12)–(14) that when the

density is low,

$$\frac{a_e^2}{2\lambda_D^2} = \frac{4\pi n m c^2}{B^2} = \frac{\omega_{pi}^2}{\omega_{HB}^2} < 1,$$

the frequency and wavelength are characterized by  $\omega_{pi}$  and  $\lambda_D$ , while for high density they are characterized by  $\omega_{HB}$  and  $a_e$ .

#### B. Modified Two-Stream Instability, $k_z \neq 0$

If the gradients are weak, the instability presented above competes with a modified two-stream instability. Neglecting the gradients in (4), but retaining a small component of  $k$  parallel to the magnetic field,

$$|k_x(T_e/m)^{1/2}| < |\omega + k_y cE/B|,$$

and expanding the denominator of the electron integral in  $k_x$ , the dispersion relation (4) becomes (taking  $k_1 a_e \ll 1$ ,  $k_x \ll k_1$ )

$$1 + \frac{4\pi n m c^2}{B^2} - \frac{\omega_{pi}^2}{\omega^2} - \frac{k_x^2}{k_1^2} \frac{\omega_{pe}^2}{(\omega - k_y v_E)^2} = 0 \quad (15)$$

under the approximations described above.

Note that the usual condition for the two-stream instability<sup>22</sup>  $v_E > (T_e/m)^{1/2}$  is replaced by the much weaker condition  $v_E > (k_x/k)(T_e/m)^{1/2}$ . Because the magnetic field limits thermal motions across  $B$  to a distance  $a_e$ , electrostatic waves with longer wavelength  $k_1 a_e < 1$ , propagating nearly perpendicular to  $B$ , see the electrons as a *cold* fluid, even if the drift (and wave) speed is much less than the true thermal speed of the electrons. Another point of view is that  $k_{||} \ll k_1$  produces a wave whose phase velocity along  $B$ , where the electrons are free to move, exceeds the thermal speed, but whose speed in the direction of the drift (perpendicular to  $B$ , where the electrons do not spread thermally) is of the same magnitude as the drift speed, even when  $v_E \ll (T_e/m)^{1/2}$ .

Equation (15) is solved by the same techniques<sup>22</sup> as for the field-free two-stream instability. Choosing  $k_x$  and  $k_1$  to maximize the growth rate and still satisfy the restrictions above gives

$$\begin{aligned} \omega_R \approx \gamma_{\max} &\approx \left[ \omega_{pi} / \left( 1 + \frac{4\pi n m c^2}{B^2} \right)^{1/2} \right] \left( \frac{v_E}{c_s} \right)^{1/5}, \\ k_y \lambda_D &\sim (c_s/v_E)^{2/5} \left( 1 + \frac{4\pi n m c^2}{B^2} \right)^{-1/2}, \\ (k_x/k_1) &\sim (m/M)^{1/2} (v_E/c_s)^{3/5}. \end{aligned} \quad (16)$$

The expansion in  $k_1 a_e$  and  $k_x$  limits the calculation to drifts above the ion sound speed, while ion damping stabilizes the mode for drifts below the ion thermal speed; thus

$$v_E > [(T_e + T_i)/M]^{1/2} \quad (17)$$

is required for instability. Note that the frequency

and growth rate of this mode scale with density in the same way as the mode discussed above in Sec. III A 1, and essentially the same stabilization criterion (17) obtains for the two modes. Both are quite happy growing a  $T_e \approx T_i$  plasma.

#### IV. NUMERICAL RESULTS

In order to both verify the approximate analytic results presented in Sec. III, to extend the results to parameter ranges where analytic solutions cannot be obtained, and especially to find the effects of finite electron and ion temperature, we have solved the dispersion relations Eqs. (4) and (6) for the drift-wave branch ( $k_x = 0$ ) in a variety of cases. These solutions employ a routine due to Barberio-Corsetti<sup>23</sup> to calculate the plasma dispersion function  $Z(\lambda)$ .

##### A. Dependence on $k$ ; $T_i \rightarrow 0$

This range was explored analytically in Sec. III for both weak ( $v_E v_\Delta \ll c_s^2$ ) and strong ( $v_E v_\Delta \gtrsim c_s^2$ ) drifts, where solutions to Eq. (6) for maximum growth rate were given. We have solved (6) numerically to find the dependence of  $\omega_R$  and  $\gamma$  on wave number  $k_y$ , retaining specifically only a density gradient so that

$$v_\Delta = \frac{-T_e}{m\omega_{ce}} \frac{1}{n_e} \frac{dn_e}{dx}.$$

Note, however that for  $k^2 a_e^2 \ll 1$ , density and magnetic gradients enter in the same way so that a selected value of  $v_\Delta$  from Eq. (8) includes a variety of gradient combinations.

Figure 3(a) shows the frequency and growth rate as a function of  $k$  for weak drift ( $v_E v_\Delta \ll c_s^2$ ). Different curves show various combinations of  $E \times B$  drift ( $v_E$ ) and gradient-produced velocity ( $v_\Delta$ ) with the total velocity of the electrons relative to the ions kept fixed at  $c_s$ , the acoustic speed. Triangles are analytic results from Eqs. (9)–(11).

Figure 3(b) shows the frequency and growth rate as a function of  $k$  for the transition between the weak ( $v_E v_\Delta \ll c_s^2$ ) and strong ( $v_E v_\Delta > c_s^2$ ) drift. The ratio  $v_\Delta/v_E$  is held fixed at  $\frac{1}{3}$ , and  $v_E/c_s$  is varied. This is the parameter range in which no analytic solution could be obtained. Triangles are analytic results for the weak drift ( $v_E v_\Delta \ll c_s^2$ ), Eqs. (9)–(11). Squares are analytic results for the strong drift ( $v_E v_\Delta \gtrsim c_s^2$ ), Eqs. (12)–(14).

Figure 3(c) shows the frequency and growth rate as a function of  $k$  for strong drift ( $v_E v_\Delta \gtrsim c_s^2$ ), with various combinations of  $v_E$  and  $v_\Delta$  but fixed  $v_\Delta + v_E = 10c_s$ . Squares are analytic results from Eqs. (12)–(14). Note for this low-density case [ $A = (8\pi n m c^2/B^2)^{1/2} = 0.1$ ] frequencies are characterized by  $\omega_{pi}$  and wavelengths by  $\lambda_D$ .

Figure 4 shows the effect of changing  $A = (8\pi n m c^2/B^2)^{1/2}$  for an intermediate-strength

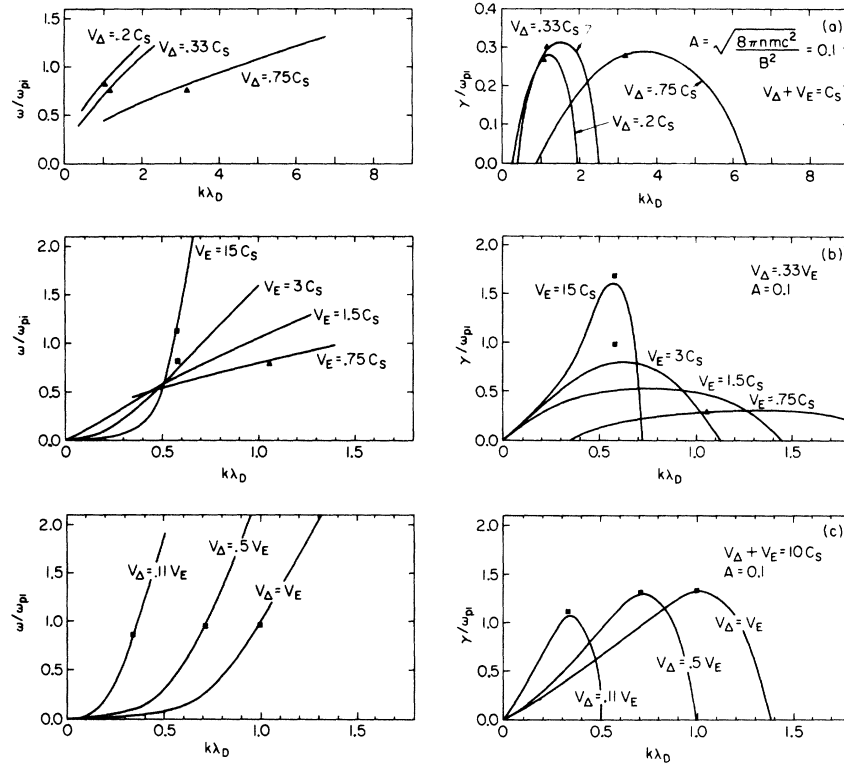


FIG. 3. Numerical solutions to Eq. (6). (a) Weak drift. Triangles are analytic results. (b) Transition between weak and strong drift. Triangle is the analytic result for  $v_E = 0.75c_s$ . Squares are analytic results for the strong drift for  $v_E = 3c_s$  and  $v_E = 15c_s$ . (c) Strong drift.

drift ( $v_E v_\Delta = \frac{3}{4} c_s$ ), with  $v_E = 1.5c_s$  and  $v_\Delta = 0.5c_s$ . No analytic expression is available for this case.

Analytic results for maximum growth rates for the high-density and strong-drift case ( $v_E v_\Delta > c_s^2$ ) are contained in Sec. III, Eqs. (12)–(14). Because of the approximation  $I_0(b) \approx 1 - b$ , these are valid only for  $v_\Delta \ll v_E$ , since for high density  $\frac{1}{2} k^2 a_e^2 \approx v_\Delta / v_E$ , and thus the corrections for finite gyro-radius become important for  $v_\Delta \sim v_E$ . Figure 5 shows the numerical solutions of (6) for frequency and growth rate as a function of  $k$  for various gradient-produced velocities  $v_\Delta$  for a fixed sum  $v_E + v_\Delta = 10c_s$ , and shows the breakdown of the  $ka_e \ll 1$  approximation. Analytic results, shown by triangles, correspond to Eqs. (12)–(14).

#### B. Temperature Ratio and Drift-Speed Thresholds for Drift-Wave Instability

In order to investigate the effects of electron-ion temperature ratios, Eq. (4) with  $k_x = 0$  and

$$\alpha = -\frac{1}{T_e} \frac{dT_{\perp e}}{dx} = 0$$

was solved numerically without further approximation. Thus both finite electron and ion temperatures

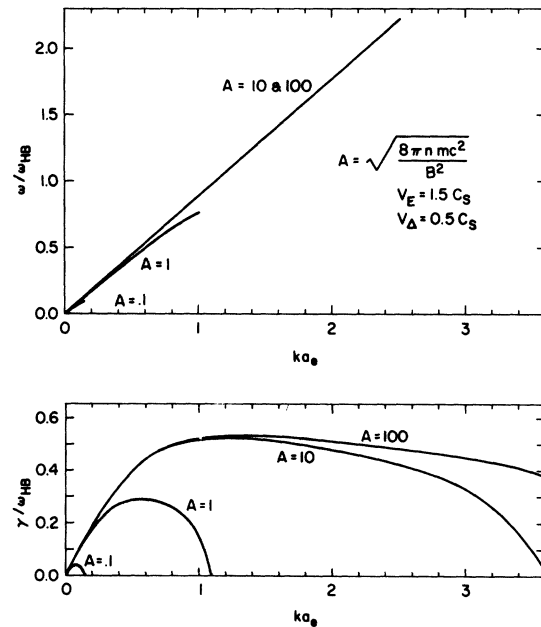


FIG. 4. Effect of changing density  $A = (8\pi n m c^2 / B^2)^{1/2}$  for an intermediate drift. Curves are numerical solutions of Eq. (6).

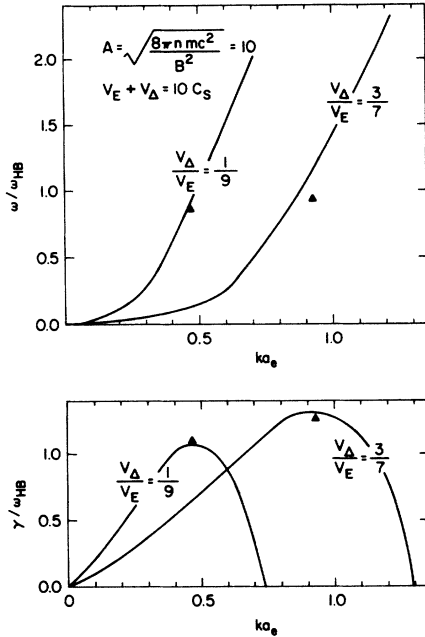


FIG. 5. Numerical solutions to Eq. (6) for high density  $8\pi nmc^2 \gg B^2$  and a strong drift. Analytic results break down when  $v_\Delta \sim v_E$  as discussed in the text.

are included in these results. Figure 6 shows that the instability persists with large growth rates even for  $T_e \ll T_i$ . However, Fig. 6(c) shows that the range of unstable wave numbers becomes increasingly small as  $T_e$  is reduced far below  $T_i$ . The analytic results from Eqs. (12)–(14) shown by squares in Fig. 6 are too high when  $T_e < T_i$  as expected: Neglect of ion damping is not fully justified since for the parameters in Fig. 6,  $kv_i/\omega > \frac{1}{2}$  for  $T_e < T_i$ .

If the electrons are colder than the ions so that  $c_s < v_i$ , then the important parameter in determining stability is the ratio of the drift speed  $v_E$  to the ion thermal velocity  $v_i$ , rather than  $v_E/c_s$ . Figure 7 shows the growth rate as a function of  $v_E/v_i$ . It can be seen that the growth rate becomes insignificant for  $v_E \lesssim v_i$ . If the result of this instability is to heat ions, as discussed elsewhere,<sup>24</sup> the limiting ion temperature should correspond to  $v_i \approx v_E$ .

#### C. Numerical Results for Instabilities in Plasmas with No Pressure

$$\text{Gradient, } \frac{1}{n_e T_e} \frac{dn_e T_{1e}}{dx} \rightarrow 0$$

Even when the pressure gradient vanishes, the magnetic gradient can drive the instability. This is seen analytically in Eq. (6). However, as shown in Sec. III A, the approximations leading to (6) breakdown with increasing electron temperature. We therefore have solved Eq. (4) numerically in this case, including the effect of finite temperature.

The result is summarized by Fig. 8 which shows the maximum growth rate as a function of  $\beta = 4\pi n T_e / B^2$ ; the squares show the analytic estimates (12)–(14). The growth rates are significant only when  $\beta$  is small,  $\beta < 0.2$ .

#### V. CONCLUSIONS

We conclude that in addition to the intermediate frequency waves which require either strong beams [ $v_E > (T_e/m)^{1/2}$ ] or hot electrons ( $T_e \gg T_i$ ) for growth, there are a number of modes, described above, which are unstable with large growth rates

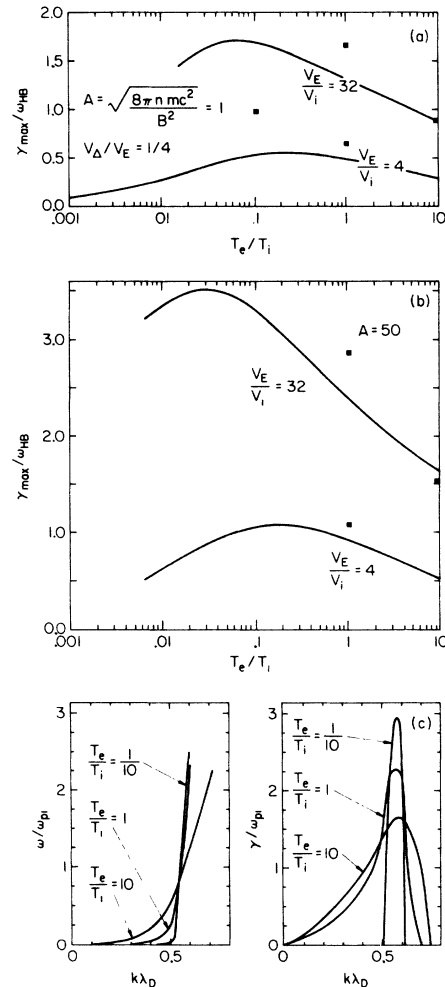


FIG. 6. Finite electron and ion temperature effects. These curves are numerical solutions to Eq. (4) with  $k_x = 0$  and no temperature gradient. (a) and (b) Maximum growth rate plotted against temperature ratio. Analytic results (squares) are too high for  $T_e < T_i$ . (c) Frequency and growth rate as a function of wave number. Note that as  $T_e/T_i$  decreases, the range of unstable  $k$  decreases. For (c),  $v_E = 32v_i$ ,  $v_D = 0.25v_E$ , and  $A = 0.1$ .



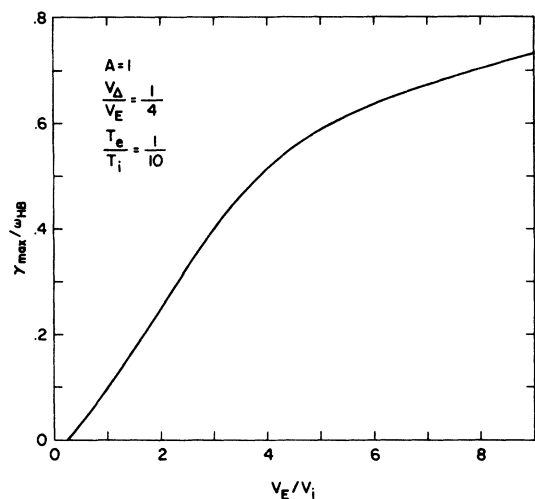


FIG. 7. Maximum growth rate as a function of  $v_E/v_i$ . As the drift speed approaches the ion thermal speed, the growth rate becomes insignificant.

even when the electrons are cool ( $T_e \leq T_i$ ) and drifts moderate ( $v_E > [(T_e + T_i)/M]^{1/2}$ ). Because of the hydrodynamic nature of these modes we expect that they will have a strong influence on the macroscopic properties of geometries in which they grow. They would be expected in magnetic collision-free shock waves,<sup>1-5</sup> magnetic pulse-diffusion experiments,<sup>3</sup> and other experiments involving electric fields perpendicular to the confining magnetic field.<sup>20</sup> Although the nonlinear aspects of these modes are still being explored, they have already been invoked to explain a number of features (ion

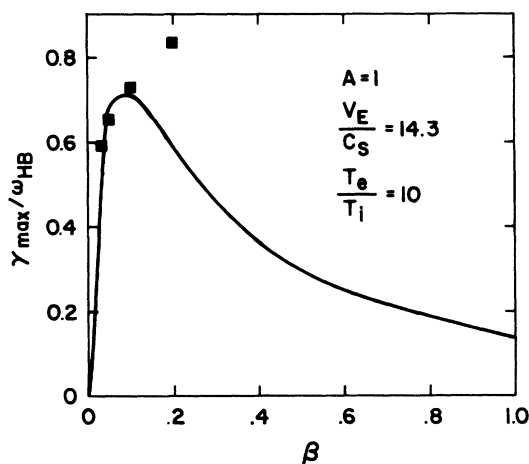


FIG. 8. Maximum growth rate as a function of  $\beta$  for a plasma with no pressure gradient. Curve is the numerical solution to Eq. (4). Squares are analytic results for the strong drift with  $v_{\Delta} = (T_e/m\omega_{ce})(1/B)dB/dx = \beta v_E$ . Note the breakdown of the low- $\beta$  approximation, as predicted.

heating, turbulent fields) of several such experiments.<sup>12,24</sup>

#### ACKNOWLEDGMENTS

Portions of this paper are based on the thesis research of one of the authors (P. C. L.) in partial fulfillment of the requirements for the Degree of Doctor of Philosophy at the University of Maryland. This research was supported in part by the Computer Science Center of the University of Maryland and in part by the Office of Naval Research.

<sup>1</sup>J. W. Paul, C. C. Daughney, and L. S. Holmes, *Nature* **216**, 363 (1967).

<sup>2</sup>S. G. Alikhanov, N. I. Alinuskii, G. G. Dolgov-Savelev, B. G. Eseevich, R. Kh. Kurtmullaev, V. K. Malinuskii, Yu. E. Nesterikhin, V. I. Pilskii, R. Z. Sagdeev, and V. N. Semenov, 1968 Novosibirsk Conference Report No. CN24/A-1, Culham Translation CTO/533 (unpublished).

<sup>3</sup>A. W. DeSilva, D. F. Duchs, G. C. Goldenbaum, H. R. Griem, E. A. Hintz, A. C. Kolb, H.-J. Kunze, and I. M. Vitkovitsky, *Plasma Physics and Controlled Nuclear Fusion Research* (IAEA, Vienna, 1969), Vol. 1, p. 143.

<sup>4</sup>M. Keilhacker, M. Kornherr, and H. H. Steuer, *Z. Physik* **223**, 385 (1969).

<sup>5</sup>D. A. Tidman and N. A. Krall, *Shock Waves in Collisionless Plasma* (Wiley, New York, 1971), Chap. 7.

<sup>6</sup>N. A. Krall and D. L. Book, *Phys. Rev. Letters* **23**, 574 (1969).

<sup>7</sup>R. Z. Sagdeev and A. A. Galeev, *Nonlinear Plasma Theory* (Benjamin, New York, 1969), pp. 94-103.

<sup>8</sup>S. P. Gary, *J. Plasma Phys.* **4** (No. 4), 753 (1970).

<sup>9</sup>S. P. Gary, and J. Sanderson, *J. Plasma Phys.* **4** (No. 4) 739 (1970).

<sup>10</sup>Dr. E. Hintz has emphasized this important point in

numerous discussions during the past several years.

<sup>11</sup>A. B. Mikhailovskii and V. S. Tsypin, *Zh. Eksperim i Teor. Fiz. Pis'ma v Redaktitsya* [Sov. Phys. JETP Letters] **3**, 158 (1966).

<sup>12</sup>W. Davis, A. W. DeSilva, W. Dove, H. R. Griem, N. A. Krall, and P. C. Liewer, Proceedings of the 1971 IAEA Conference of Plasma Physics and Controlled Nuclear Fusion Research, Madison, Wisconsin, 1971 (unpublished).

<sup>13</sup>N. A. Krall and D. L. Book, *Phys. Fluids* **12**, 347 (1969).

<sup>14</sup>N. A. Krall, in *Advances in Plasma Physics*, edited by A. Simon and W. B. Thompson [Interscience, New York, 1968], Vol. 1, p. 162.

<sup>15</sup>N. K. Bajaj and N. A. Krall, *Phys. Fluids* (to be published).

<sup>16</sup>N. K. Bajaj (private communication).

<sup>17</sup>H. V. Wong, *Phys. Fluids* **13**, 757 (1970).

<sup>18</sup>D. W. Forslund, R. L. Morse, and C. W. Nielson, *Phys. Rev. Letters* **25**, 1266 (1970).

<sup>19</sup>M. Lampe, W. M. Manheimer, J. B. McBride, J. H. Orens, R. Shanny, and R. N. Sudan, *Phys. Rev. Letters* **17**, 1221 (1971).

<sup>20</sup>S. E. Segre and M. Martone, *Plasma Phys.* **13**, 133 (1971).

<sup>21</sup>I. Alexeff, K. Estabrook, A. Hirose, W. D. Jones, R. V. Neidigh, J. N. Olsen, F. R. Scott, W. L. Stirling, M. M. Widner, and W. R. Wing, *Phys. Rev. Letters* 25, 848 (1970).

<sup>22</sup>T. Stix, *The Theory of Plasma Waves* (McGraw-Hill,

New York, 1962), pp. 129-130.

<sup>23</sup>P. Barberio-Corsetti, Princeton Plasma Physics Report No. MATT-773, 1970 (unpublished).

<sup>24</sup>N. A. Krall and P. C. Liewer, University of Maryland Technical Report No. 71-107 (unpublished).